AIMS Mathematics, 8(5): 11095–11112.
DOI: 10.3934/math.2023562
Received: 07 January 2023
Revised: 10 February 2023
Accepted: 17 February 2023
Published: 09 March 2023

http://www.aimspress.com/journal/Math

*Research article*

# The stresses components in position and time of weakened plate with two holes conformally mapped into a unit circle by a conformal mapping with complex constant coefficients

**Sharifah E. Alhazmi[1], M. A. Abdou[2,*] and M. Basseem[3]**

[1] Department of Mathematics, Al-Qunfudah University College, Umm Al-Qura University, Mecca, Kingdom of Saudi Arabic
[2] Department of Mathematics, Faculty of Education, Alexandria University, Egypt
[3] Department of Mathematics, Faculty of Engineering, Sinai University, Egypt

* **Correspondence:** Email: abdella_777@yahoo.com.

**Abstract:** In this paper, an infinite elastic plate weakened by two holes are considered and the complex variable method is used to derive a closed form of Gaursat functions for the first and second fundamental problems with variant time. The holes, in all previous works, are conformally mapped outside the unit circle without time. Here, the two holes are conformally mapped into the unit circle $\varpi$ in the effect of time by the generalized rational mapping function with complex constant coefficients. By using this conformal mapping function, the fundamental problems transfer to an integro-differential equation with Cauchy kernel. Then, after applying the complex variable method, one can obtain a closed form of Gaursat functions. Some applications were discussed and the time effect on the applications was studied. In addition, the different stress components in each application have also been calculated using Maple 2022.1.

**Keywords:** an infinite plate; Gaursat functions; conformal mapping; elastic plane; complex variable method; curvilinear hole
**Mathematics Subject Classification:** 30C20, 74B99

## 1. Introduction

For plate structural components that contain holes under the action of external loads, there is often a greater stress concentration around the holes. Therefore, accurately calculating the stresses on the edge of the holes is playing an important role in evaluating the stability and strengthening of the structure. As for the complex variable method proposed by Muskhelishvili [1], it is particularly suitable for the previous problems in which the regions can be conformally mapped to circles or rings. Haddon [2] used this method to obtain the solution of an infinite plate containing two holes under uniaxial tension. Lu et al. [3] applied a conformal transformation in complex function to discuss the solution of an elastic plate problem containing two holes with an internal traction along the holes. Zeng et al. [4] discussed the stress and tension effect on an elastic infinite plate bounded by two oval holes. A closed-form plane strain solution was presented, for stresses and displacements around tunnels, by Exadaktylos and Stavropoulos [5]. Abdou et al. [6–8] discussed the stresses and the strains components for infinite plates weakened by different curvilinear holes conformally mapped outside the unit circle using different conformal mappings. In the problems of cracks, in the two-dimensional elasticity, there are two types of cracks. The first type has a longitudinal crack in the range [−1, 1], and this type generates several types of integral equations with singular kernel in one of the forming forms:
(i) weak singular kernel logarithmic kernel $k(u,v) = ln|u-v|$, and Carleman function $k(u,v) = |u-v|^{-\alpha}$, 0<α<1.
(ii) For the kernel $k(u,v) = \frac{1}{(u-v)^m}$ at $m = 1$, we have Cauchy kernel, strong kernel at $m = 2$ and super strong kernel at $m > 2$.

These types of equations can be solved using different analytic or numerical methods. Zachariah et al. [9] investigated the application of Aramid/Carbon fiber reinforced polymer hybrid thin laminate in enhancing static and dynamic transverse loading behavior. Gonenli and Das [10] presented the effect of cracks on free vibration response for circular and annular thin plates. Lal et al. [11] studied the effect of various discontinuities like voids, soft inclusions and hard inclusions of the mixed-mode stress intensity factor, crack growth and energy release rate of an edge crack isotropic plate under different loading by various numerical examples. More information for the solution of singular integral equation with Cauchy kernel can be found in the works of Badr [12], Duruk et al. [13] and Abdou et al. [14,15]. The second type, is represented by an elastic plate with a curvilinear hole, in the complex plane in the theory of elasticity, the curvilinear hole can be transformed inside or outside the unit circle or in the half plane. In this case the potential functions are called Gaursat functions.

Muskhelishvili [1] solved the problem of stretching an infinite plate weakened by an elliptic hole by using the transformation.

$$z = c(\zeta + m\zeta^{-1}). \tag{1.1}$$

This transformation conformally maps the infinite domain bounded internally by an elliptic onto the domain outside the unit circle $|\zeta| = 1$ in the $\zeta -$ plane.

In this paper, we focused the problem where an infinite plate weakened by two different holes, see Figure 1.

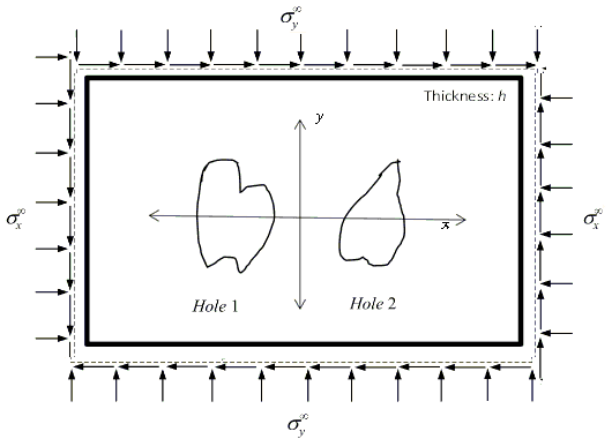


**Figure 1.** Two different holes in an infinite plate.

In this paper, we use a new mapping function in the fundamental problems of an infinite plate with two arbitrary different holes. Moreover, an analytical stress solution for an elastic infinite plate with two such holes, which is subjected to a uniform tension and external forces, is derived using a complex variable method. In addition, as a new study, we consider different materials to obtain its Gaursat functions with fixed time. Then, we discuss and investigate the change of stress components of an infinite plate under uniform tension and external forces for variant time.

## 2. Gaursat functions and stress components

Consider the conformal mapping

$$z = w(\zeta) = A + \frac{B}{\zeta} + \frac{C\zeta}{1-n_1\zeta} + \frac{D\zeta}{1-n_2\zeta}, \quad |\zeta| < 1, \ (n_1 \neq n_2), \tag{2.2}$$

where A, B, C, and D are complex constants.

The conformal mapping (2.2) transforms the two holes into the interior of a unit circle. In addition, this form is considered a more general and comprehensive form than what was studied in the paper [16]. Moreover, the mapping (2.2) satisfies the condition $(w(0), w\left(\frac{1}{n_1}\right), w\left(\frac{1}{n_2}\right)) \neq 0$, inside the unit circle by taking $B = 0, C = 0, D = 0$, respectively.

Abodu and Basseem [16], take the first and second fundamental problems of potential functions with time effects in the form

$$\kappa\Phi_1(z,t) - z\overline{\frac{\partial\Phi_1(z,t)}{\partial z}} - \overline{\Psi_1(z,t)} = f(z,t), \tag{2.3}$$

where, for the first fundamental problem $\kappa = -1$, $f(z,t)$, there is a given function of stresses. While, for the second fundamental problem $\kappa = \frac{\lambda+3\mu}{\lambda+\mu} > 1, \lambda = \frac{E\nu}{(1+\nu)(1-2\nu)}$ and $\mu = G = \frac{E}{2(1+\nu)}$ are called Lame's constants, $E$ is the Young's modulus and G is the modulus of shear. In this case, $f(z,t)$ represents the strain function.

In this case, the two complex functions $\Phi_1(z,t)$ and $\Psi_1(z,t)$ take the formations (Abdou and Basseem [16])

$$\Phi_1(z,t) = -\frac{R_x(t)+iR_y(t)}{2\pi(1+\kappa)}\ln\zeta + \zeta\Gamma(t) + \Phi(\zeta,t), \tag{2.4}$$

$$\Psi_1(z,t) = -\frac{\kappa\left(R_x(t)-iR_y(t)\right)}{2\pi(1+\kappa)}\ln\zeta + \zeta\Gamma^*(t) + \Psi(\zeta,t),\ (0 \le t < 1). \tag{2.5}$$

Here $\{R_x(t),\ R_y(t)\}$ are the components of the resultant vector of all external forces in time acting on the boundary, $\{\Gamma(t),\ \Gamma^*(t)\}$ are complex functions in time, the two complex functions $\{\Psi(\zeta,t), \Phi(\zeta,t)\}$ are analytic and called Gaursat functions.

In this case, the stress components take the forms

$$\sigma_{xx} = Re\left[2\frac{\partial\Phi(\zeta,t)}{\partial z} - \bar{z}\frac{\partial^2\Phi(z,t)}{\partial z^2} + \frac{\partial\Psi(z,t)}{\partial z}\right], \tag{2.5}$$

$$\sigma_{yy} = Re\left[2\frac{\partial\Phi(\zeta,t)}{\partial z} + \bar{z}\frac{\partial^2\Phi(z,t)}{\partial z^2} + \frac{\partial\Psi(z,t)}{\partial z}\right], \tag{2.6}$$

and

$$\sigma_{xy} = Im\left[\bar{z}\frac{\partial^2\Phi(z,t)}{\partial z^2} - \frac{\partial\Psi(z,t)}{\partial z}\right]. \tag{2.7}$$

## 3. Conformal mapping and special cases

### *3.1. Conformal mapping*

The parametric equations are obtained from Eq (2.2) as $x = \mathrm{Re}(z)$ and $\mathrm{y} = \mathrm{Im}(z)$. For different $\{\mathrm{n}_1,\ \mathrm{n}_2\}$ and $\{\mathrm{A}, \mathrm{B}, \mathrm{C}, \mathrm{D}\}$, we get the following new shapes

### *3.2. Special cases*

(i) Figures 2 and 3 describe the conformal mapping (2.2) for different real values of $\mathrm{n}_1, \mathrm{n}_2, \mathrm{A}, \mathrm{B}, \mathrm{C}$ and D. We also notice that the figures are symmetrical around $x$ and $y$ axes.

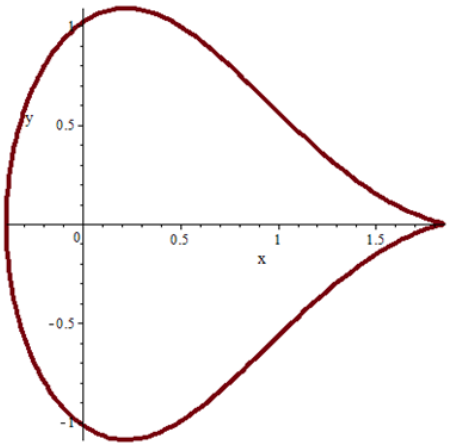


**Figure 2.** $\mathrm{n}_1 = 0.4,\ \mathrm{n}_2 = 0.1; \mathrm{A} = 5.00,\ \mathrm{B} = 1.00,\ \mathrm{C} = 1.53,\ \mathrm{D} = -6.03.$

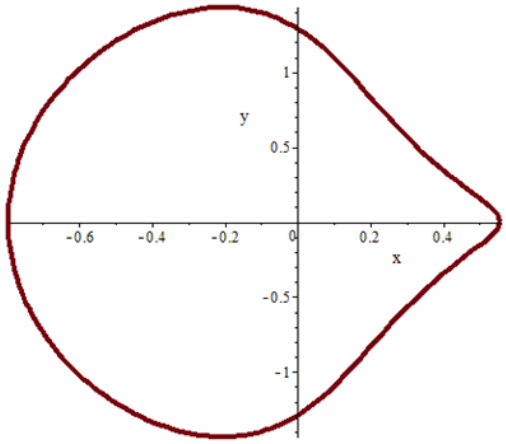


**Figure 3.** $n_1 = 0.6,\ n_2 = 0.1; A = 5.00,\ B = 1.00,\ C = 0.24, D = -5.443.$

(ii) For $n_1 = n_2 = 0, A = 0,$ we get $Z = (C + D)\zeta + B\zeta^{-1}$ which is discussed in Muskelishvilis [1].

(iii) By taking $A = 0, B = 1$ and $n_1C + n_2D = -1 + n_1n_2$ where $(n_1 + n_2) = C + D,$ the boundary curvilinear holes degenerate into a circular cut having strong pole. This singularity can be removed by taking$(n_1 + n_2) < C + D,$ see Figures 4 and 5. If $n_1 = 0$ or $n_2 = 0,$ see Figures 6 and 7.

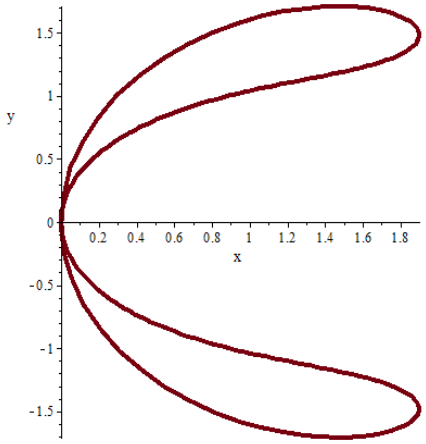


**Figure 4.** $n_1 = 0.6,\ n_2 = 0.3; A = 0.00,\ B = 1.00,\ C = -2.13,\ D = 3.03.$

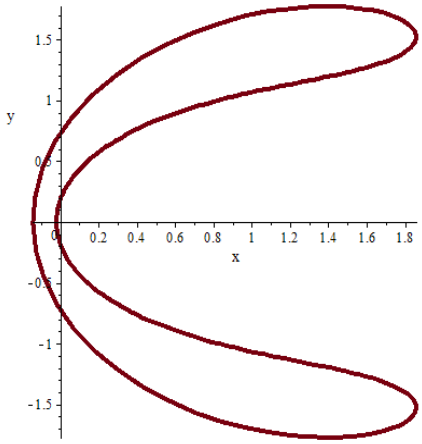


**Figure 5.** $n_1 = 0.6,\ n_2 = 0.3;\ A = 0.00,\ B = 1.00,\ C = -2.213,\ D = 3.073.$

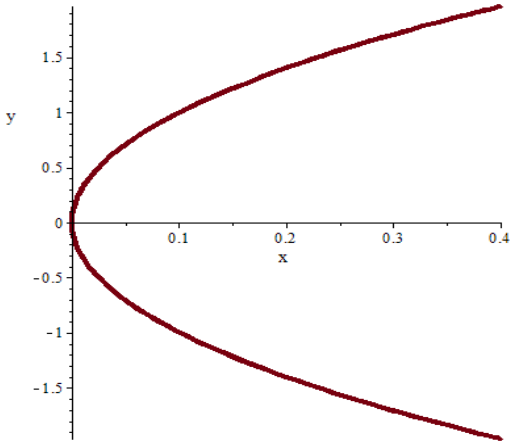


**Figure 6.** $n_1 = 0.0,\ n_2 = 0.2;\ A = 0.00,\ B = 1.00,\ C = -4.8,\ D = 5.0.$

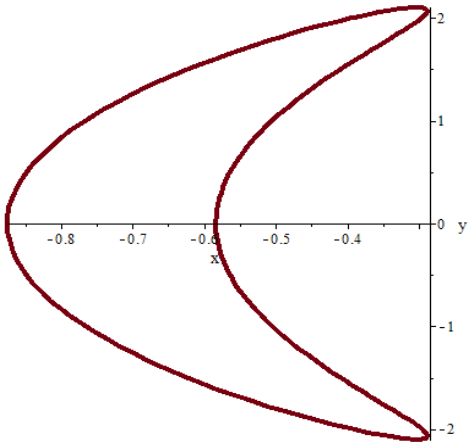


**Figure 7.** $n_1 = 0.2,\ n_2 = 0.0;\ A = 0.00,\ B = 1.00,\ C = -5.5,\ D = 5.0.$

(iv) Taking $n_2 = 0$, $A = 0$, $C + D = n_1 B$ and let $m = -\frac{n_1 D}{B}$, we get $z = B\frac{\zeta^{-1}+m\zeta}{1-n_1\zeta}$, see

Figures 8 and 9.

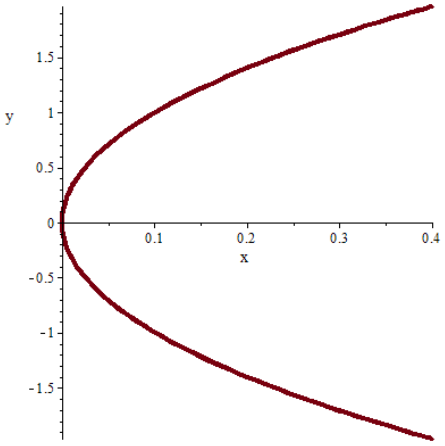


**Figure 8.** $n_1 = 0.1,\ n_2 = 0.0;\ A = 0.00,\ B = 1.00,\ C = 7.1,\ D = -7.$

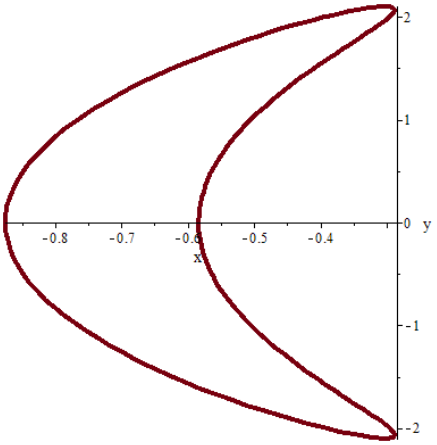


**Figure 9.** $n_1 = 0.3,\ n_2 = 0.0;\ A = 0.00,\ B = 1.00,\ C = -\frac{11}{30},\ D = \frac{2}{3}.$

(v) In all previous shapes, symmetric about x-axis, the constants are real. While when it is complex, the shapes are anomalous, see Figures 10–13.

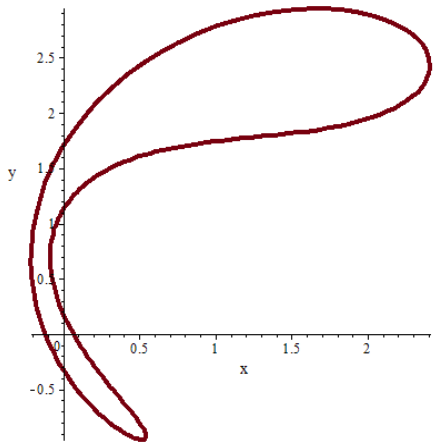


**Figure10.** $n_1 = 0.352,\ n_2 = 0.3;\ A = 0.947 + 2.84i,\ B = 1,\ C = -6.58 + 22.4i,$ $D = 6.289 - 24.376i.$

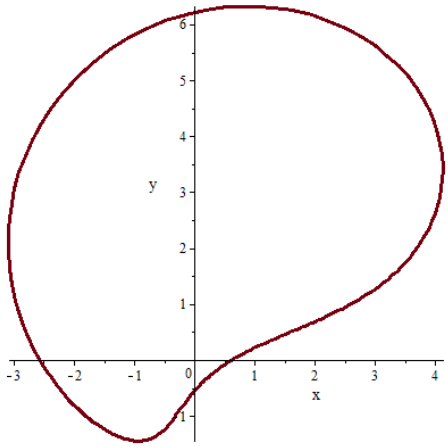


**Figure 11.** $n_1 = 0.3,\ n_2 = 0.5;\ A = 13.3i,\ B = 0.7,\ C = 1.6 - 18.3i,\ D = -1.2 + 5.9i.$

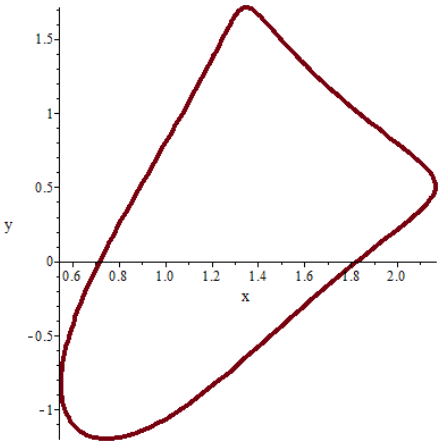


**Figure 12.** $n_1$=0.352, $n_2$=0.2i; A=-4.26i, B=1, C=1.164+0.66i, D=0.088+3.8i.

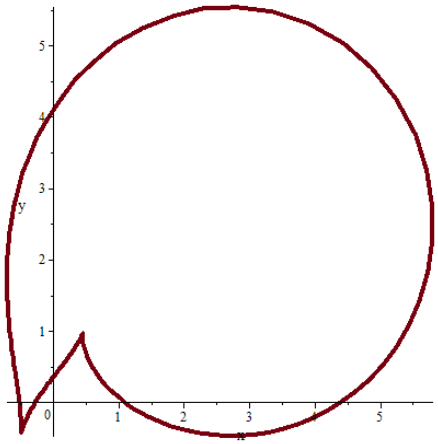


**Figure 13.** $n_1 = 0.7 + 0.07i$, $n_2 = 0.02 + 0.5i$; $A = -0.11 - 1.843i$, $B = 0.7$, $C = 1.43 + 1.94i$, $D = -0.719 + 0.616i$.

## 4. Method of solution

Using the transformation mapping of Eq (1.2), then Eq (2.3) is transformed into an integro-differential equation in complex position and time, which has anomaly Cauchy kernel in the imaginary plane, then applying the complex variable method with the residue theorems to obtain a closed expression for Gaursat functions.

For this, consider

$$\frac{w(\zeta)}{w'(\zeta)} = \xi_1(\zeta) + \xi_2(\zeta) + \varrho(\zeta) \tag{4.8}$$

where $\{\xi_1(\zeta), \xi_2(\zeta)\}$ are singular parts and $\varrho(\zeta)$ is a regular function, in which

$$\xi_i = \frac{h_i}{1-n_i\zeta}, i = 1, 2 \tag{4.9}$$

where

$$h_i = \frac{(\alpha + \beta n_i + \gamma n_i^2 + \eta n_i^3)(1 - n_i\, n_j)^2\,(1 - n_i^2)^2}{\chi_i(n_i - n_j)}, \{i, j\} = \{1, 2\},\ i \neq j, \tag{4.10}$$

$$\chi_i = \left(1 - n_i n_j\right)(1 - n_i^2)\left(2\alpha n_i^2 + \beta n_i - \frac{\eta}{n_i}\right) -$$

$$(\alpha + \beta n_i^2 + \gamma n_i + \eta)\left(2n_i^2 n_j - n_i - n_j\right), \tag{4.11}$$

and

$$\alpha = An_1n_2, \beta = -A(n_1 + n_2) + n_1n_2B - n_2C - n_1D,$$
$$\gamma = A - (n_1 + n_2)B + C + D, \eta = B. \tag{4.12}$$

Using Eqs (4.8), (2.4) and (2.5) in Eq (1.2), we get

$$\kappa\Phi(\zeta,t) - (\xi_1 + \xi_2)\overline{\frac{\partial\Phi(\zeta,t)}{\partial\zeta}} - \overline{\Psi_*(\zeta,t)} = f_*(\zeta,t), \tag{4.13}$$

where

$$\Psi_*(\zeta,t) = \Psi(\zeta,t) + \overline{\varrho(\zeta)}\,\frac{\partial\Phi(\zeta,t)}{\partial\zeta}, \tag{4.14}$$

$$f_*(\zeta,t) = f(\zeta,t) + \kappa\zeta\Gamma(t) + \overline{\frac{\Gamma^*(t)}{\zeta}} + (\xi_1 + \xi_2 + \varrho)\mathrm{N}(\zeta,t), \tag{4.15}$$

and

$$N(\zeta,t) = \overline{\Gamma(t)} - \frac{\mathrm{R}_x(\zeta,t) - iR_y(\zeta,t)}{2\pi(1+\kappa)}\,\zeta, |\zeta| < 1. \tag{4.16}$$

Equation (4.13) represents singular equations of the first and second fundamental problems that can be solved using Cauchy method. For this, multiply Eq (4.13) by $\frac{1}{2\pi i(\zeta-\sigma)}$ and integrate it with respect to σ on ϖ. So, we have

$$\kappa\Phi(\zeta,t) - \frac{n_1h_1b_1(t)}{1-n_1\zeta} - \frac{n_2h_2b_2(t)}{1-n_2\zeta} = A(\zeta,t) - \kappa\zeta\Gamma(t) + \frac{n_1h_1N\left(\frac{1}{n_1},t\right)}{1-n_1\zeta} + \frac{n_2h_2N\left(\frac{1}{n_2},t\right)}{1-n_2\zeta}, \tag{4.17}$$

where

$$\frac{1}{2\pi i}\oint_{\varpi}\frac{f(\sigma,t)}{\zeta-\sigma}\,d\sigma = A(\zeta,t), \tag{4.18}$$

and

$$\frac{1}{2\pi i}\oint_{\varpi}\frac{[\xi_1(\sigma)+\xi_2(\sigma)]\overline{\frac{\partial\Phi(\sigma,t)}{\partial\sigma}}}{\zeta-\sigma}\,d\sigma = \frac{n_1h_1b_1(t)}{1-n_1\zeta} + \frac{n_2h_2b_2(t)}{1-n_2\zeta}, \tag{4.19}$$

where $b_1(t)$ and $b_2(t)$ are complex functions that will be determined, such that $b_1(0) = b_2(0) = 0$. Differentiate (4.17) with respect to $\zeta$ and using the result of $\overline{\frac{\partial\Phi(\zeta,t)}{\partial\zeta}}$ in (4.19), we get

$$\left(\overline{\frac{\partial A(\zeta,t)}{\partial\zeta}}\right)_{\zeta=\frac{1}{n_i}} - \kappa\overline{\Gamma(t)} + \frac{\overline{n_i^2h_iN\left(\frac{1}{n_i},t\right)}}{(1-n_i^2)^2} + \frac{\overline{n_j^2\,h_jN\left(\frac{1}{n_j},t\right)}}{\left(1-n_in_j\right)^2} + \frac{\overline{n_i^2h_ib_i(t)}}{(1-n_i^2)^2} + \frac{\overline{n_j^2h_jb_j(t)}}{\left(1-n_in_j\right)^2} = kb_i(t),$$

$$\{i,j\} = \{1,2\},\ i \neq j. \tag{4.20}$$

Solving for $b_i(t)$ and $\overline{b_i(t)}$, $i = \{1,2\}$, then substitute the results in (4.19), so that $\Phi(\zeta,t)$ is completely determined. The second Gaursat function can be obtained where

$$\Psi(\zeta,t) = \kappa\overline{\Phi(\zeta,t)} - (\overline{\xi 1 + \xi 2 + \varrho})\frac{\partial\Phi(\zeta,t)}{\partial\zeta} - f_*(\zeta,t), \tag{4.21}$$

Equations (4.17) and (4.21) represent the Gaursat functions. After obtaining it, the stresses components of Eqs (2.5) and (2.6) can be determined.

## 5. Applications

In this section, the numerical results and tables were computed using Maple 2022.1 software, Version 15, March 2022, Windows, 10, 8 G RAM, 64-bi.

(5.i) The first fundamental problem for an infinite plate under the effect of uniform tensile stresses: Assume an elastic plate of thickness h and having two holes such that the components of the resultant external forces $X(x,t) = Y(y,t) = 0, (\forall t \in [0,1), \kappa = -1$. Assume stresses tensile $\Gamma(t) = \frac{P(t)}{4}$ and $\Gamma^*(t) = -\frac{P(t)}{2} e^{-2i\theta}$, where $P(t) = \frac{1+t}{4(1-t)}, t < 1, \theta = \frac{\pi}{4}$ and the known function of stress$f(z,t) = 0$. Under the above assumptions, we have the first fundamental problem in the absence of the stress function $f(z,t) = 0$. In this case, the problem represents an infinite plate stretched at infinity by the application of uniform tensile stress of intensity $P(t)$ making an angle $\theta$ with the x-axis. The plate is weakened by curvilinear holes which are free from stresses. The following Figures 14–19 represent the stress components with a time variant where $n_1 = 0.1$ and $n_2 = 0.6$ in Eq (2.2).

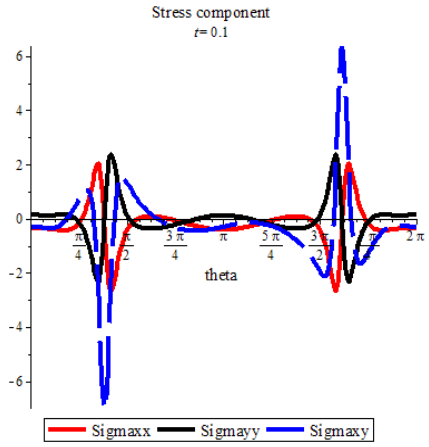


**Figure 14.** Stress components where $t = 0.1$.

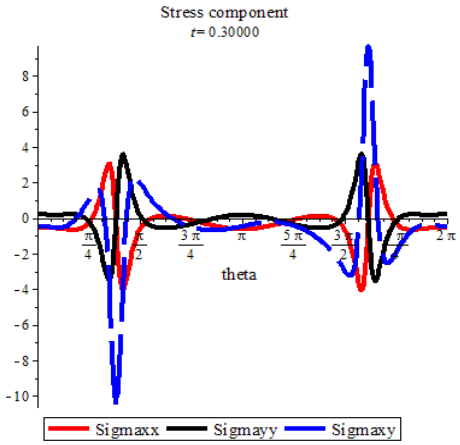


**Figure 15.** Stress components where $t = 0.3$.

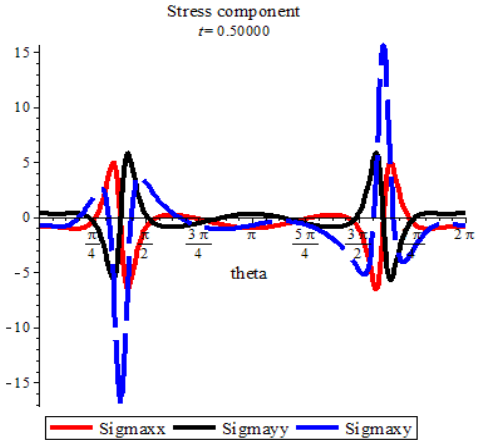


**Figure 16.** Stress components where $t = 0.5$.

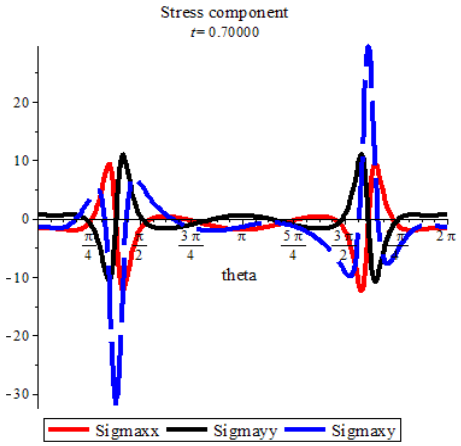


**Figure 17.** Stress components where $t = 0.7$.

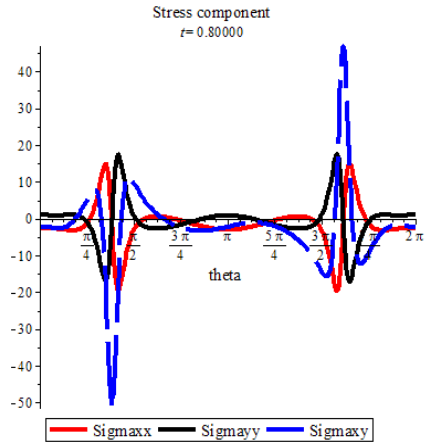


**Figure 18.** Stress components where $t = 0.8$.

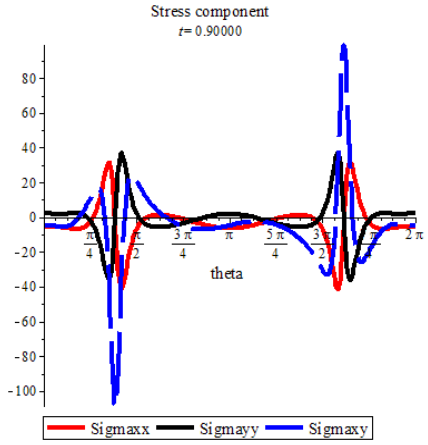


**Figure 19.** Stress components where $t = 0.9$.

(5.ii) For $\kappa = -1$, $\mathrm{X(x,t)} = \mathrm{Y(y,t)} = \Gamma(\mathrm{t}) = \Gamma^*(t) = 0$, $f(z,t) = zP(t)$ and $P(t) = \frac{1+t}{4(1-t)}$, $t < 1$, we have the first fundamental problem and the stress function $f(z,t)$ takes the variable form in position and time and the pressure is variable in time only. In this case, we have an infinite plate that is weakened by curvilinear holes, when there are no external forces and the edges of holes are subject to a uniform pressure. The stress ratio $\frac{\sigma_{xx}}{\sigma_{yy}}$, is shown by the following Figures 20 and 21 for variant $t$ and $\theta$.

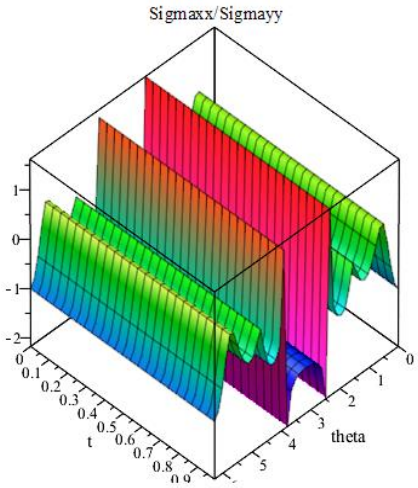


**Figure 20.** Stress ratio where $\mathrm{n}_1 = 0.4$, $\mathrm{n}_2 = 0.1$.

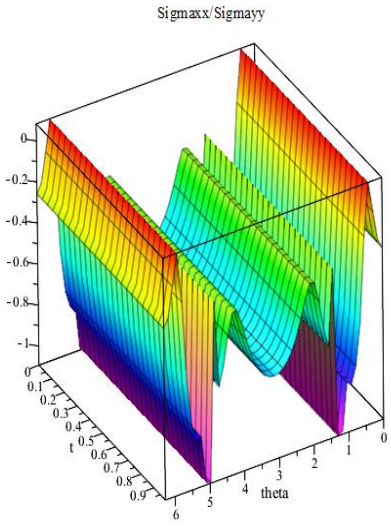


**Figure 21.** Stress ratio where $n_1 = 0.6$, $n_2 = 0.1$.

(5.iii) When increasing $\kappa = \frac{\lambda+3\mu}{\lambda+\mu} > 1, \lambda$ and $\mu$ are called Lame's constants, and for different materials with fixed time, $t = 0.3$, in the presence of external forces $X = 900$ unit, $Y = 750$ unit and $\Gamma(t) = \Gamma^*(t) = f(z,t) = 0$, we have the second fundamental problem in the absence of strain function. In this case, the absolute values of Gaursat functions at time $t = 0.3$ are shown by Table 1.

**Table 1.** $|\Phi(\zeta, 0.3)|$ and $|\Psi(\zeta, 0.3)|$ where $X = 900\,unit$, $Y = 750\,unit$, $\Gamma = \Gamma^* = 0$, $n_1 = 0.6$, $n_2 = 0.1$, $A = 5.00$, $B = 1.00$, $C = 0.24$ and $D = -5.443$ where $|.| = \sqrt{Re^2(.) + Im^2(.)}$.

| Material name | $E\ (GPa)$ | $\nu$ | $\kappa$ | $\theta$ | $\lvert\Phi\rvert$ | $\lvert\Psi\rvert$ |
|---|---|---|---|---|---|---|
| | | | | 0 | 26.97980821 | 19.39650117 |
| | | | | 22/35 | 17.93291537 | 90.33109568 |
| | | | | 66/35 | 9.943618450 | 148.4923859 |
| Lead | 13-15 | 0.44 | 1.239 | 22/7 | 8.696292743 | 41.73803367 |
| | | | | 22/5 | 10.08031449 | 146.3944312 |
| | | | | 198/35 | 18.22009620 | 124.3672333 |
| | | | | 44/7 | 26.97858407 | 19.26310140 |
| | | | | 0 | 17.13329406 | 16.57564982 |
| | | | | 22/35 | 11.41190680 | 79.52754127 |
| | | | | 66/35 | 6.335287463 | 126.0476143 |
| Copper | 121-130 | 0.35 | 1.64 | 22/7 | 5.533946715 | 35.40707464 |
| | | | | 22/5 | 6.402571164 | 124.8312640 |
| | | | | 198/35 | 11.55685907 | 101.2446494 |
| | | | | 44/7 | 17.13265384 | 16.49154699 |
| | | | | 0 | 14.68592663 | 15.65936561 |
| | | | | 22/35 | 9.787359429 | 75.76579721 |
| | | | | 66/35 | 5.434980103 | 118.8661378 |
| Iron | 204-212 | 0.3 | 1.8 | 22/7 | 4.745875368 | 33.38591745 |
| | | | | 22/5 | 5.487971518 | 117.8636508 |
| | | | | 198/35 | 9.902615855 | 94.38228069 |
| | | | | 44/7 | 14.68541084 | 15.58745606 |

(5.iv) Taking the iron material, $\kappa = 1.8$, in the presence of external forces $X(z,t) = 900e^t$, $Y(z,t) = 750e^t$ and $\Gamma = \Gamma^* = f = 0$ .The application describes the second fundamental problem when the external forces are variable in time, while the tensions $\Gamma, \Gamma^*$ $and$ the strain function $f$(z,t) are absent, for all values of time. The absolute values of Gaursat functions with time variant are shown by Table 2.

**Table 2.** $|\Phi(\zeta,t)|$ and $|\Psi(\zeta,t)|$ where $X = 900e^t$, $Y = 750e^t$, $\Gamma = \Gamma^* = 0$, $n = 0.3$, $B = 1$, $A = nB$, $C - An = 0.7$ and $\kappa = 1.8$.

| $t$ | $\Theta$ | $\lvert\Phi(\zeta,t)\rvert$ | $\lvert\Psi(\zeta,t)\rvert$ |
|---|---|---|---|
| | 0 | 14.78839018 | 15.76862084 |
| | 22/35 | 9.855645727 | 76.29441435 |
| | 66/35 | 5.472899900 | 119.6954655 |
| 0.007 | 22/7 | 4.778987287 | 33.61885064 |
| | 22/5 | 5.526261035 | 118.6859842 |
| | 198/35 | 9.971706292 | 95.04078480 |
| | 44/7 | 14.78787078 | 15.69620957 |
| | 0 | 15.74333793 | 16.78686616 |
| | 22/35 | 10.49206569 | 81.22106147 |
| | 66/35 | 5.826307769 | 127.4246988 |
| 0.07 | 22/7 | 5.087586339 | 35.78975941 |
| | 22/5 | 5.883114656 | 126.3500310 |
| | 198/35 | 10.61562077 | 101.1779628 |
| | 44/7 | 15.74278500 | 16.70977899 |
| | 0 | 29.43445432 | 31.38548174 |
| | 22/35 | 19.61643901 | 151.8545580 |
| | 66/35 | 10.89312766 | 238.2389611 |
| 0.7 | 22/7 | 9.511980772 | 66.91414762 |
| | 22/5 | 10.99933638 | 236.2297138 |
| | 198/35 | 19.84744316 | 189.1668806 |
| | 44/7 | 22.84416758 | 31.24135608 |

## 6. Discussion and conclusions

From the above results and discussion we can establish the following:

(1) The transformation mapping of two holes $z = w(\zeta) = A + \frac{B}{\zeta} + \frac{C\zeta}{1-n_1\zeta} + \frac{D\zeta}{1-n_2\zeta}$, $|\zeta| < 1$ transforms the curvilinear two holes into the domain inside the unit circle under the conditions $w(0)$, $w\left(\frac{1}{n_1}\right), w\left(\frac{1}{n_2}\right) \neq 0$.

(2) The engineering benefit of using the mapping transform function comes from its various forms when handling holes. This mapping function deals with famous shapes of tunnels and studying stresses around it, see Exadaktylos et al. [5, 17].

(3) The positive values of stresses means that they act as a tension forces, while its negative values means the stresses act as a pressure forces.

(4) From Figures 14 – 19, we deduce that $max\ \sigma_{xx} = -min\sigma_{yy}$ and stress components increase with time.

(5) When the vertical stress on the $y-$axis takes its maximum value and displays the treatments of the internal resistance of the body (such as rocks for example), while the vertical stress, on the $x-$axis, is small according to the $y-$axis. At this point, it is best to treat the problem in points determined by the angles that give $\frac{\sigma_{xx}}{\sigma_{yy}}$ to its minimum values in a certain time, see Figures 20 and 21.

(6) Time effect: Figure 22, illustrates the stresses by varying the time for arbitrary value of θ. In this situation we infer that the stresses rapidly rise with time and that the maximum time must be lower than one unit.

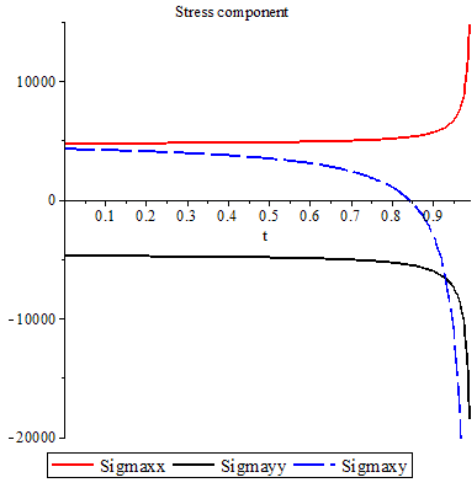


**Figure 22.** Stresses components with time effect where $n_1 = 0.6$, $n_2 = 0.1$, $\theta = \frac{3\pi}{8}$.

Among the difficulties that we faced while conducting this research, include the following:

(1) How to obtain Gaursat functions in the presence of a magnetic field. We have set this research as a future study.

(2) We believe that there are a lot of applications in real life beside crack problems in tunnels or caves. In biomathematics, they can be used to treat leaf holes caused by pests and to protect plants. Therefore, as a future study, we can use Gaursat functions as a mathematical model for healing and treating burns and wounds.

**Acknowledgments**

We would like to thank the reviewers for their suggestions that helped improve the research. We thank the Deanship for Research & Innovation, Ministry of Education in Saudi Arabia for funding this research through the project number: IFP22UQU4282396DSR050.

**Conflict of interest**

We declare that there are no conflicts of interest regarding the publication of this paper.

## References


[1] N. Muskhelishvili, *Some basic problems of mathematical theory of elasticity*, Dordrecht: Springer, 1977. https://doi.org/10.1007/978-94-017-3034-1

[2] R. Haddon, Stresses in an infinite plate with two unequal circular holes, *The Quarterly Journal of Mechanics and Applied Mathematics*, **20** (1967), 277–291. https://doi.org/10.1093/qjmam/20.3.277

[3] A. Lu, Z. Xu, N. Zhang, Stress analytical solution for an infinite plane containing two holes, *Int. J. Mech. Sci.*, **128** (2017), 224–234. https://doi.org/10.1016/j.ijmecsci.2017.04.025

[4] X. Zeng, A. Lu, N. Zhang, Analytical stress solution for an infinite plate containing two oval holes, *Eur. J. Mech. A-Solid.*, **67** (2018), 291–304. https://doi.org/10.1016/j.euromechsol.2017.09.011

[5] G. Exadaktylos, M. Stavropoulou, A closed form elastic solution for stress and displacement around tunnels, *Int. J. Rock Mech. Min.*, **39** (2002), 905–916. https://doi.org/10.1016/S1365-1609(02)00079-5

[6] M. Abdou, Fundamental problems for infinite plate with a curvilinear hole having finite poles, *Appl. Math. Comput.*, **125** (2002), 79–91. https://doi.org/10.1016/S0096-3003(00)00117-X

[7] M. Abdou, S. Asseri, Goursat functions for an infinite plate with a generalized curvilinear hole in zeta plane, *Appl. Math. Comput.*, **212** (2009), 23–36. http://dx.doi.org/10.1016/j.amc.2009.01.079

[8] M. Abdou, A. Jann, An infinite elastic plate weakened by a generalized curvilinear hole and Goursat functions, *Applied Mathematics*, **5** (2014), 728–743. https://doi.org/10.4236/am.2014.54070

[9] S. Zachariah, S. Shenoy, D. Pai, Experimental analysis of the effect of the woven aramid fabric on the strain to failure behavior of plain weaved carbon/aramid hybrid laminates, *Facta Univ.-Ser. Mech.*, in press. https://doi.org/0.22190/FUME200819022Z

[10] C. Gonenli, O. Das, Free vibration analysis of circular and annular thin plates based on crack characteristics, *Reports in Mechanical Engineering*, **3** (2022), 158–167. https://doi.org/10.31181/rme20016032022g

[11] A. Lal, M. Vaghela, K. Mishra, Numerical analysis of an edge crack isotropic plate with void/inclusions under different loading by implementing XFEM, *J. Appl. Comput. Mech.*, **7** (2021), 1362–1382. https://doi.org/10.22055/jacm.2019.31268.1848

[12] A. Bader, Integro-differential equation with Cauchy kernel, *J. Comput. Appl. Math.*, **134** (2001), 191–199. https://doi.org/10.1016/S0377-0427(00)00536-7

[13] N. Duruk, H. Erbay, A. Erkip, Global existence and blow-up for a class of nonlocal nonlinear Cauchy problems arising in elasticity, *Nonlinearity*, **23** (2010), 107–118. http://dx.doi.org/10.1088/0951-7715/23/1/006

[14] M. Abdou, S. Raad, S. AlHazmi, Fundamental contact problem and singular mixed integral equation, *Life Sci. J.*, **11** (2014), 323–329.

[15] M. Abdou, A. Jaan, On a computational method for solving nonlinear mixed integral equation with singular kernel, *J. Comput. Theor. Nanos.*, **13** (2016), 2917–2923. https://doi.org/10.1166/jctn.2016.4938

[16] M. Abdou, M. Basseem, Thermopotential function in position and time for a plate weakened by curvilinear hole, *Arch. Appl. Mech.*, **92** (2022), 867–883. https://doi.org/10.1007/s00419-021-02078-x

[17] G. Exadaktylos, P. Liolios, M. Stavropoulou, A semi-analytical elastic stress-displacement solution for notched circular openings in rocks, *Int. J. Solids Struct.*, **40** (2003), 1165–1187. https://doi.org/10.1016/S0020-7683(02)00646-7


AIMS Press